

Ab initio shell model with a genuine three-nucleon force for the *p*-shell nuclei

Petr Navrátil and W. Erich Ormand

Lawrence Livermore National Laboratory, L-414, P.O. Box 808, Livermore, CA 94551

The *ab initio* no-core shell model (NCSM) is extended to include a realistic three-body interaction in calculations for *p*-shell nuclei. The NCSM formalism is reviewed and new features needed in calculations with three-body forces are discussed in detail. We present results of first applications to ${}^6,7\text{Li}$, ${}^6\text{He}$, ${}^{7,8,10}\text{Be}$, ${}^{10,11,12}\text{B}$, ${}^{12}\text{N}$ and ${}^{10,11,12,13}\text{C}$ using the Argonne V8' nucleon-nucleon (NN) potential and the Tucson-Melbourne TM'(99) three-nucleon interaction (TNI). In addition to increasing the total binding energy, we observe a substantial sensitivity in the low-lying spectra to the presence of the realistic three-body force and an overall improvement in the level-ordering and level-spacing in comparison to experiment. The greatest sensitivity occurs for states where the spin-orbit interaction strength is known to play a role. In particular, with the TNI we obtain the correct ground-state spin for ${}^{10,11}\text{B}$ and ${}^{12}\text{N}$, ${}^{12}\text{B}$, contrary to calculations with NN potentials only.

PACS numbers: 21.60.Cs, 21.45.+v, 21.30.-x, 21.30.Fe

I. INTRODUCTION

The *ab initio* no-core shell model (NCSM) [1] is a method to solve the nuclear structure problem for light nuclei considered as systems of A nucleons interacting by realistic inter-nucleon forces. The calculations are performed using a large but finite harmonic-oscillator (HO) basis. Due to the basis truncation, it is necessary to derive an effective interaction from the underlying inter-nucleon interaction that is appropriate for the basis employed. The effective interaction contains, in general, up to A -body components even if the underlying interaction had, e.g. only two-body terms. In practice, the effective interaction is derived in a sub-cluster approximation retaining just two- or three-body terms. A crucial feature of the method is its convergence to exact solution with increasing basis size and/or an increase in the effective interaction clustering.

In the past, applications were limited to only realistic two-nucleon interactions. However, the recent introduction of the capability to derive a three-body effective interaction [2] and apply it in either relative-coordinate [3] or Cartesian-coordinate [4] formalism together with the ability to solve a three-nucleon system with a genuine three-nucleon force in the NCSM approach [5] opens the possibility to include a realistic three-nucleon interaction (TNI) in the NCSM Hamiltonian and perform calculations for the *p*-shell nuclei.

We note that there are several methods that can be used to solve the $A = 3, 4$ systems with realistic Hamiltonians that include a realistic three-body interaction. However, until now, only the Green's function Monte Carlo (GFMC) method [6, 7, 8, 9] is capable to obtain solution for light *p*-shell nuclei with a Hamiltonian that includes both realistic two- and three-nucleon force.

In this paper, we introduce an extension of the NCSM formalism to accommodate the TNI and present first applications for several *p*-shell nuclei. The main purpose of this paper is to introduce the formalism needed to perform *ab initio* shell-model calculations for the *p*-shell nuclei with Hamiltonians that include a realistic three-nucleon interaction. At the same time, we present a snapshot of first applications for several *p*-shell nuclei of different masses with the primary goal of assessing a general impact of a realistic TNI on the structure of different *p*-shell nuclei. In this study, we limit ourselves to the use of a single TNI, the chiral-symmetry based Tucson-Melbourne TM'(99) [10], combined with the Argonne V8' NN potential [6]. More detailed studies using a broader variety of realistic three-nucleon interactions will follow in the future.

In Section II, the extension of the NCSM formalism to include realistic three-nucleon forces is discussed. In Section III, we present first results obtained with Hamiltonians that include the Tucson-Melbourne TM'(99) TNI for ${}^6,7\text{Li}$, ${}^6\text{He}$, ${}^{7,8,10}\text{Be}$, ${}^{10,11,12}\text{B}$, ${}^{12}\text{N}$ and ${}^{10,11,12,13}\text{C}$. Some overall observations of the effect of the TNI are gathered in Section IV. Finally, we summarize our conclusions in Section V.

II. AB INITIO NO-CORE SHELL MODEL WITH A THREE-NUCLEON FORCE

A detailed description of the NCSM approach was presented, e.g. in Refs. [1, 2, 3]. Here, we emphasize extensions and modifications needed when a genuine TNI is included. In the case when the TNI is considered, the starting

Hamiltonian is

$$H_A = \frac{1}{A} \sum_{i < j} \frac{(\vec{p}_i - \vec{p}_j)^2}{2m} + \sum_{i < j} V_{\text{NN},ij} + \sum_{i < j < k} V_{\text{NNN},ijk}, \quad (1)$$

where m is the nucleon mass, $V_{\text{NN},ij}$, the NN interaction with both strong and electromagnetic components, $V_{\text{NNN},ijk}$ the three-nucleon interaction. In the NCSM, we employ a large but finite harmonic-oscillator (HO) basis. Due to properties of the realistic nuclear interaction in Eq. (1), we must derive an effective interaction appropriate for the basis truncation. To facilitate the derivation of the effective interaction, we modify the Hamiltonian (1) by adding to it the center-of-mass (CM) HO Hamiltonian $H_{\text{CM}} = T_{\text{CM}} + U_{\text{CM}}$, where $U_{\text{CM}} = \frac{1}{2} A m \Omega^2 \vec{R}^2$, $\vec{R} = \frac{1}{A} \sum_{i=1}^A \vec{r}_i$. The effect of the HO CM Hamiltonian will later be subtracted out in the final many-body calculation. Due to the translational invariance of the Hamiltonian (1) the HO CM Hamiltonian has in fact no effect on the intrinsic properties of the system in the infinite basis space. The modified Hamiltonian can be cast into the form

$$\begin{aligned} H_A^\Omega &= H_A + H_{\text{CM}} = \sum_{i=1}^A h_i + \sum_{i < j} V_{ij}^{\Omega,A} + \sum_{i < j < k} V_{\text{NNN},ijk} \\ &= \sum_{i=1}^A \left[\frac{\vec{p}_i^2}{2m} + \frac{1}{2} m \Omega^2 \vec{r}_i^2 \right] + \sum_{i < j} \left[V_{\text{NN},ij} - \frac{m \Omega^2}{2A} (\vec{r}_i - \vec{r}_j)^2 \right] + \sum_{i < j < k} V_{\text{NNN},ijk}. \end{aligned} \quad (2)$$

Next we divide the A -nucleon infinite HO basis space into the finite active space (P) comprising of all states of up to N_{max} HO excitations above the unperturbed ground state and the excluded space ($Q = 1 - P$). The basic idea of the NCSM approach is to apply a unitary transformation on the Hamiltonian (2), $e^{-S} H_A^\Omega e^S$ such that $Q e^{-S} H_A^\Omega e^S P = 0$. If such a transformation is found, the effective Hamiltonian that exactly reproduces a subset of eigenstates of the full space Hamiltonian is given by $H_{\text{eff}} = P e^{-S} H_A^\Omega e^S P$. This effective Hamiltonian contains up to A -body terms and to construct it is essentially as difficult as to solve the full problem. Therefore, we apply this basic idea on a sub-cluster level. When a genuine TNI is considered, the simplest approximation is a three-body effective interaction approximation. The NCSM calculation is then performed with the following four steps:

(i) We solve a three-nucleon system for all possible three-nucleon channels characterized by a fixed angular momentum, isospin and parity with the Hamiltonian (2), i.e., using

$$\mathcal{H}_3 = h_1 + h_2 + h_3 + V_{12}^{\Omega,A} + V_{13}^{\Omega,A} + V_{23}^{\Omega,A} + V_{\text{NNN},123}. \quad (3)$$

Note that in Eq. (3), $A > 3$ corresponding to the investigated nucleus is kept in $V_{ij}^{\Omega,A}$, $i, j \equiv 123$ as defined in (2). Consequently, the three nucleons feel a pseudo-mean field of the spectator nucleons generated by the HO CM potential. It is necessary to separate the three-body effective interaction contributions from the TNI and from the two-nucleon interaction. Therefore, we need to find three-nucleon solutions for the Hamiltonian with and without the $V_{\text{NNN},123}$ TNI term. The three-nucleon solutions are obtained by procedures described in Refs. [2, 3] (without TNI) and [5] (with TNI). In particular, we note that we use two-body effective interaction corresponding to a very large three-nucleon basis space, i.e., up to $N_{\text{max}}^{(3)} = 40$, to obtain these solutions. The number of three-nucleon channels to include in the calculations is restricted by the maximal active space N_{max} to be used in the final A -nucleon calculation.

(ii) We construct the unitary transformation corresponding to the choice of the active basis space P_3 from the three-nucleon solutions using the Lee-Suzuki procedure [11, 12, 13, 14]. In particular, we demand that $Q_3 e^{-S} \mathcal{H}_3 e^S P_3 = 0$. Let us remark that the definition of the three-nucleon active space P_3 is determined by the definition of the A -nucleon active space P . The P_3 states contains all three-nucleon states up to the highest possible three-nucleon excitation, which can be found in the P space of the A -nucleon system. For example, for $A = 6$ and $N_{\text{max}} = 6$ ($6\hbar\Omega$) space we have P_3 defined by $N_{3\text{max}} = 8$. Similarly, for the p -shell nuclei with $A \geq 7$ and $N_{\text{max}} = 6$ ($6\hbar\Omega$) space we have $N_{3\text{max}} = 9$. We note that the anti-hermitian transformation operator S can be expressed as [14]

$$S = \text{arctanh}(\omega - \omega^\dagger), \quad (4)$$

with the operator ω satisfying $\omega = Q_3 \omega P_3$. If the eigensystem of the Hamiltonian \mathcal{H}_3 (3) is given by $\mathcal{H}_3 |k\rangle = E_k |k\rangle$, then the operator ω can be determined from

$$\langle \alpha_Q | \omega | \alpha_P \rangle = \sum_{k \in \mathcal{K}} \langle \alpha_Q | k \rangle \langle \tilde{k} | \alpha_P \rangle, \quad (5)$$

where the tilde denotes the inverse of the matrix defined by matrix elements $\langle \alpha_P | k \rangle$, i.e., $\sum_{\alpha_P} \langle \tilde{k} | \alpha_P \rangle \langle \alpha_P | k' \rangle = \delta_{k,k'}$ and $\sum_k \langle \alpha'_P | \tilde{k} \rangle \langle k | \alpha_P \rangle = \delta_{\alpha'_P, \alpha_P}$, for $k, k' \in \mathcal{K}$. In Eq. (5), $|\alpha_P\rangle$ and $|\alpha_Q\rangle$ are the active-space and the Q -space basis

states, respectively, and \mathcal{K} denotes a set of d_P eigenstates, whose properties are reproduced in the P -space, with d_P equal to the dimension of the P -space. The set \mathcal{K} is typically chosen by selecting the lowest three-nucleon eigenstates for the given three-nucleon channel. In practice, to calculate the P -space matrix elements of the effective Hamiltonian, we apply the Eqs. (15) and (16) of Ref. [1]. The three-body effective interaction is then obtained as

$$V_{3\text{eff},123}^{\text{NN+NNN}} = P_3 \left[e^{-S_{\text{NN+NNN}}} (h_1 + h_2 + h_3 + V_{12}^{\Omega,A} + V_{13}^{\Omega,A} + V_{23}^{\Omega,A} + V_{\text{NNN},123}) e^{S_{\text{NN+NNN}}} - (h_1 + h_2 + h_3) \right] P_3 \quad (6)$$

and

$$V_{3\text{eff},123}^{\text{NN}} = P_3 \left[e^{-S_{\text{NN}}} (h_1 + h_2 + h_3 + V_{12}^{\Omega,A} + V_{13}^{\Omega,A} + V_{23}^{\Omega,A}) e^{S_{\text{NN}}} - (h_1 + h_2 + h_3) \right] P_3. \quad (7)$$

Note that we distinguish the transformation $S_{\text{NN+NNN}}$ corresponding to the Hamiltonian \mathcal{H}_3 (3) and the transformation S_{NN} corresponding to the Hamiltonian without the TNI term, i.e., $h_1 + h_2 + h_3 + V_{12}^{\Omega,A} + V_{13}^{\Omega,A} + V_{23}^{\Omega,A}$. The three-body effective interaction contribution from the TNI we then define as

$$V_{3\text{eff},123}^{\text{NNN}} \equiv V_{3\text{eff},123}^{\text{NN+NNN}} - V_{3\text{eff},123}^{\text{NN}}. \quad (8)$$

(iii) As the three-body effective interactions are derived in the Jacobi-coordinate HO basis but the p -shell nuclei calculations will be performed more efficiently in a Cartesian-coordinate single-particle Slater-determinant M -scheme basis, we need to perform a suitable transformation of the interactions. This transformation is a generalization of the well-known transformation on the two-body level that depend on HO Brody-Moshinsky brackets. The antisymmetrized Jacobi-coordinate HO basis in which the three-body effective interaction is obtained can be represented in the form $|NiJMTM_T\rangle$ where N is the total number of HO excitation, i is an additional quantum number enumerating the antisymmetrized states, J and T are the total three-nucleon angular momentum and isospin, respectively, and M , M_T their third components. This basis can be expanded in a $2 + 1$ nucleon cluster basis using expansion coefficients, i.e.,

$$|NiJMTM_T\rangle = \sum \langle (nlsjt, \mathcal{N}\mathcal{L}\frac{1}{2}\mathcal{J}\frac{1}{2}) || NiJT \rangle | (nlsjt, \mathcal{N}\mathcal{L}\frac{1}{2}\mathcal{J}\frac{1}{2}) JMTM_T \rangle, \quad (9)$$

where the $|nl\rangle$ HO state describes relative motion of nucleon 1 and 2, $|\mathcal{N}\mathcal{L}\rangle$ describes the relative motion of the third nucleon with respect to the CM of nucleons 1 and 2, and $\langle (nlsjt, \mathcal{N}\mathcal{L}\frac{1}{2}\mathcal{J}\frac{1}{2}) || NiJT \rangle$ is the coefficient of fractional parentage. It holds that $N = 2n + l + 2\mathcal{N} + \mathcal{L}$. For further details and the procedure how to calculate the expansion coefficients see Ref. [3]. The basis for the three-body effective interaction suitable for the shell-model code input is a three-nucleon Slater-determinant HO basis characterized by $M_3 = m_{j_1} + m_{j_2} + m_{j_3}$, $M_T = m_{t_1} + m_{t_2} + m_{t_3}$ and parity, formed by the single particle states $|nl\frac{1}{2}jm_j\frac{1}{2}m_t\rangle$ that depend on the single-particle coordinates. We introduce a short-hand notation for these Slater-determinant states, i.e., $|(nl\frac{1}{2}jm_j\frac{1}{2}m_t)_{(abc)}\rangle$, where a, b, c labels the occupied states. In order to transform the three-body effective interaction to the new basis we need first to couple the relative coordinate basis (9) with the three-nucleon CM HO states $|N_{\text{CM}}L_{\text{CM}}M_{\text{CM}}\rangle$ to form a complete basis. The three-body effective interaction is independent on the $N_{\text{CM}}L_{\text{CM}}M_{\text{CM}}$ quantum numbers. The overlap of the two respective states can then be expressed in the form

$$\begin{aligned} & \langle (nl\frac{1}{2}jm_j\frac{1}{2}m_t)_{(abc)} | NiJMTM_T; N_{\text{CM}}L_{\text{CM}}M_{\text{CM}} \rangle = \delta_{2n_a+l_a+2n_b+l_b+2n_c+l_c, N+2N_{\text{CM}}+L_{\text{CM}}} \\ & \times \delta_{m_{j_a}+m_{j_b}+m_{j_c}, M+M_{\text{CM}}} \delta_{m_{t_a}+m_{t_b}+m_{t_c}, M_T} \sqrt{6} \sum \langle (nlsjt, \mathcal{N}\mathcal{L}\frac{1}{2}\mathcal{J}\frac{1}{2}) || NiJT \rangle \frac{1}{2} (1 - (-1)^{l+s+t}) \\ & \times (l_a m_a \frac{1}{2} m_{s_a} | j_a m_{j_a}) (l_b m_b \frac{1}{2} m_{s_b} | j_b m_{j_b}) (l_c m_c \frac{1}{2} m_{s_c} | j_c m_{j_c}) (\frac{1}{2} m_{t_a} \frac{1}{2} m_{t_b} | t m_t) (t m_t \frac{1}{2} m_{t_c} | T M_T) \\ & \times (\frac{1}{2} m_{s_a} \frac{1}{2} m_{s_b} | s m_s) (l_b m_b l_a m_a | \Lambda m_\Lambda) (L_{12} M_{12} l m_l | \Lambda m_\Lambda) (l_c m_c L_{12} M_{12} | \lambda m_\lambda) \\ & \times (L_{\text{CM}} M_{\text{CM}} \mathcal{L} M_{\mathcal{L}} | \lambda m_\lambda) (\mathcal{L} M_{\mathcal{L}} \frac{1}{2} m_{s_c} | \mathcal{J} M_{\mathcal{J}}) (l m_l s m_s | j m_j) (j m_j \mathcal{J} M_{\mathcal{J}} | J M) \\ & \times \langle n_c l_c N_{12} L_{12} \lambda | N_{\text{CM}} L_{\text{CM}} \mathcal{N} \mathcal{L} \lambda \rangle_{\frac{1}{2}} \langle n_b l_b n_a l_a \Lambda | N_{12} L_{12} n \Lambda \rangle_1, \end{aligned} \quad (10)$$

where we explicitly show the total HO quantum number conservation that also implies parity conservation, the angular momentum and isospin third component conservation. The sum goes over the expansion (9), λ , Λ , N_{12} , L_{12} and the m quantum numbers in the Clebsch-Gordan coefficients not appearing on the left-hand side. The $\langle n_1 l_1 n_2 l_2 L | n_3 l_3 n_4 l_4 L \rangle_d$ are the generalized Brody-Moshinsky brackets for two-particles of mass ratio d as defined e.g., in Ref. [15]. Sums of the Clebsch-Gordan coefficients in Eq. (10) can be re-expressed as sums of 6-j and 9-j coefficients. However, some

Clebsch-Gordan coefficients will remain as we have a magnetic quantum number dependence on the left-hand side. It should be pointed out that the overlap (10) is independent of the HO frequency Ω , and for a given N_{\max} , it needs to be calculated just once. The three-body effective interaction M -scheme matrix elements are then obtained by

$$\begin{aligned} \langle (nl\frac{1}{2}jm_j\frac{1}{2}m_t)_{(abc)} | V_{3\text{eff},123} | (nl\frac{1}{2}jm_j\frac{1}{2}m_t)_{(def)} \rangle &= \sum \langle (nl\frac{1}{2}jm_j\frac{1}{2}m_t)_{(abc)} | NiJMTM_T; N_{\text{CM}}L_{\text{CM}}M_{\text{CM}} \rangle \\ \langle NiJT | V_{3\text{eff},123} | N'i'JT \rangle &\langle N'i'JMTM_T; N_{\text{CM}}L_{\text{CM}}M_{\text{CM}} | (nl\frac{1}{2}jm_j\frac{1}{2}m_t)_{(def)} \rangle. \end{aligned} \quad (11)$$

(iv) We solve the Schrödinger equation for the A -nucleon system using the Hamiltonian

$$H_{A,\text{eff}}^{\Omega} = \sum_{i=1}^A h_i + \frac{1}{A-2} \sum_{i<j<k}^A V_{3\text{eff},ijk}^{\text{NN}} + \sum_{i<j<k}^A V_{3\text{eff},ijk}^{\text{NNN}}, \quad (12)$$

where the $\frac{1}{A-2}$ factor takes care of over-counting the contribution from the two-nucleon interaction. At this point we also subtract the H_{CM} and add the Lawson projection term $\beta(H_{\text{CM}} - \frac{3}{2}\hbar\Omega)$ to shift the spurious CM excitations. Just as the bare interaction is translationally invariant, so is the effective interaction, and the energies of the physical eigenstates corresponding to the $0\hbar\Omega$ excitation of the CM are independent on the choice of β . The A -nucleon calculation is then performed using either the Many-Fermion Dynamics shell model code [16] generalized to handle three-body interactions or using the newly developed code REDSTICK [17], using a different algorithm for evaluating the Hamiltonian matrix elements, with the Hamiltonian in the form:

$$H_{A,\text{eff}}^{\Omega,\text{SM}} = \sum_{i<j}^A \left[\frac{(\vec{p}_i - \vec{p}_j)^2}{2Am} + \frac{m\Omega^2}{2A} (\vec{r}_i - \vec{r}_j)^2 \right] + \frac{1}{A-2} \sum_{i<j<k}^A V_{3\text{eff},ijk}^{\text{NN}} + \sum_{i<j<k}^A V_{3\text{eff},ijk}^{\text{NNN}} + \beta(H_{\text{CM}} - \frac{3}{2}\hbar\Omega). \quad (13)$$

We summarize this section by repeating that the effective interaction depends on the nucleon number A , the HO frequency Ω , and the P -space basis size defined by N_{\max} . It is translationally invariant and with $N_{\max} \rightarrow \infty$ the NCSM effective Hamiltonian approaches the starting bare Hamiltonian (1). Consequently, with the basis size increase the NCSM results become less and less dependent on the HO frequency and converge to the exact solution. Alternatively, by increasing the clustering of the effective interaction for a fixed P -space size the NCSM effective Hamiltonian approaches the exact A -nucleon effective Hamiltonian that reproduces exactly a subset of eigenstates of the starting Hamiltonian (1).

III. APPLICATION TO SELECTED p -SHELL NUCLEI

The calculations with the three-body interactions are technically and computationally intensive. When a genuine TNI is employed the step (i) from the previous section is computationally demanding. In addition, when a three-body effective interaction is used in general, the steps (iii) and (iv) are complex as well. In these first NCSM calculations with the TNI in the p -shell, we limit ourselves to the use of a single realistic interaction. In particular, we use the isospin invariant AV8' NN potential [6] that is a simplified version of the AV18 NN potential. For the TNI, we employ a version of the original Tucson-Melbourne force [18] corrected to drop a term later found to be inconsistent with the chiral-symmetry-based effective field theory TNI of two-pion range [19]. We note that there have been different strength constants (taken from pion-nucleon scattering data) suggested for this force [10, 18, 19]. We use only one particular set, i.e. the TM'(99) updated strength constants of the Tucson-Melbourne TNI that was introduced in Ref. [10]. We summarize the strength constants and other numbers employed in the present investigation in Table I. The cutoff Λ is the only parameter in the TNI and it is set to $\Lambda = 4.7$ by fitting the ${}^3\text{H}$ binding energy using the AV8' + TM'(99) interactions. We add the Coulomb potential to the Hamiltonian perturbatively, that is only in the P -space.

The NCSM calculations depend in general on the HO frequency and the basis size. The basis size is limited by the available computational resources and the algorithm development. In this paper, we were able to reach the $6\hbar\Omega$ basis space for $A = 6, 7$. For higher masses, we limited ourselves to the $4\hbar\Omega$ basis space. The optimal HO frequency is selected in the NCSM by the requirement of the least dependence of the eigenenergies on the frequency. Typically, for the p -shell nuclei we select the optimal frequency by finding the ground-state energy minimum in the largest accessible basis space. Due to the complexity of the calculations with the TNI, in this study we rely on our previous investigations done without the TNI to select the optimal frequency and perform comparative calculations with and without the TNI. More detailed frequency dependence investigations will be done later.

The steps (i) and (ii) of the calculations as described in Section II are performed using the Jacobi-coordinate many-body effective interaction code (*manyeff*) [3] extended to handle the TNI as described in Ref. [5]. When calculating

the three-body effective interaction induced by the two-nucleon potential, $V_{3\text{eff},123}^{\text{NN}}$ (7), we are able reach large three-nucleon basis spaces, e.g. $N_{\text{max}}^{(3)} = 40$, to obtain high precision three-nucleon solutions. Due to the complexity of the calculations with the TNI we were, however, limited in this work to smaller spaces, up to $N_{\text{max}}^{(3)} = 30$ [5], when the TNI was included in the Hamiltonian (3). This was sufficient to obtain the ${}^3\text{H}$ binding energy within 50 keV of the exact result, see Fig. 2 of Ref. [5]. Nevertheless, it would still be useful to further increase $N_{\text{max}}^{(3)}$ in the future. In particular because here we employ a lower HO frequency for which we expect a slower convergence than for that used in the ${}^3\text{H}$ calculations. In order to calculate the $V_{3\text{eff},123}^{\text{NNN}}$ (8) it is essential to use the same $N_{\text{max}}^{(3)}$ to obtain (6) and (7). Therefore, we performed three calculations, one up to $N_{\text{max}}^{(3)} = 40$ to calculate $V_{3\text{eff},123}^{\text{NN}}$ (7) in all relevant three-nucleon channels and two for (6) and (7) in the same basis space up to $N_{\text{max}}^{(3)} = 30$ for the three-nucleon channels up to $J = \frac{7}{2}$ to calculate $V_{3\text{eff},123}^{\text{NNN}}$ (8). We will improve on this in our future studies as also discussed in the concluding section. The step (iii) is performed by a specialized code that reads the outputs of the *manyeff* code and the step (iv) is then performed using either the Many-Fermion Dynamics shell model code [16] generalized to handle three-body interactions or using the newly developed code REDSTICK [17].

In order to get the most accurate assessment of the effect of the genuine three-nucleon interaction in the following we always compare calculation with and without the TNI using identical basis size, HO frequency and the clustering approximation, i.e., the three-body effective interaction.

We note that bare nucleon charges and unrenormalized transition operators were used in all the transition calculations presented in this paper. For some transitions, E2 in particular, the operator renormalization could be important. The operator renormalization can be calculated as outlined, e.g. in Ref. [1], and is now under development. In the Gamow-Teller transition calculations, the g_A constant was not included in the presented B(GT) values.

Finally, let us remark that all the presented calculated states in this paper are the p -shell or the $0\hbar\Omega$ dominated states. The opposite parity ($1\hbar\Omega$) and the $2\hbar\Omega$ -dominated states were investigated within the NCSM, e.g. in Refs. [1, 4, 27, 28]. Such states are not obtained at low enough energy in the basis spaces used in the present investigation. Therefore, in this paper comparison is made with experimental levels known to be predominantly of p -shell character.

A. ${}^6\text{Li}$, ${}^6\text{He}$

We investigated $A = 6$ nuclei using two-nucleon interactions in Ref. [20] and ${}^6\text{Li}$ in particular in Ref. [4] where we used three-body effective interaction derived from the AV8'. Our ${}^6\text{Li}$ results with the TNI are summarized in Table II and Fig. 1. We show the basis size dependence up to $6\hbar\Omega$ using the optimal frequency $\hbar\Omega = 14$ MeV. It is apparent from Fig. 1 that the basis size dependence is quite similar in the calculations with and without the TNI and it is important that the excitation energies of the low-lying states in particular show a good stability and a convergence pattern when the $6\hbar\Omega$ basis space is reached. At the same time we can see a significant sensitivity of the excitation spectra to the presence of the genuine three-nucleon interaction. It should be noted that the 3_1^+0 state excitation energy decreases significantly and it gets closer to experiment when the TNI is included. Also, the $3_1^+0 \leftrightarrow 2_1^+0$ splitting, which is underestimated with just a two-nucleon interaction, increases significantly. Our calculated ${}^6\text{Li}$ binding energy increases by more than 2.5 MeV when the TNI is included. With tighter binding with the TNI the point-proton radius decreases slightly similarly as the B(E2) value of the $1_1^+0 \rightarrow 3_1^+0$ transition. The ground-state quadrupole moment and the M1 transitions are not much affected, although there appears to be an improvement for the $2_1^+1 \rightarrow 1_1^+0$ M1 transition.

Our ${}^6\text{He}$ results are summarized also in Table II. Apart from increased binding energy, there are little differences between the calculations with and without the TNI. In the same table, we show the B(GT) values obtained for the ${}^6\text{He} \rightarrow {}^6\text{Li}$ ground-state to ground-state transition. Clearly, the TNI shifts the result in the right direction closer to experiment although a discrepancy still remains. Recently, Schiavilla and Wiringa found that the AV18/Urbana-IX interaction also over-predicts the ${}^6\text{He} \rightarrow {}^6\text{Li}$ B(GT) value [24]. In fact, their obtained Gamow-Teller matrix elements ($\equiv \sqrt{\text{B(GT)}}$), 2.254(5) and 2.246(10) using two types of wave functions, compare well with our result 2.283 for AV8'+TM'(99). Our corresponding AV8' result is 2.305 which is basically identical to our CD-Bonn result presented in Ref. [20].

B. ${}^7\text{Li}$, ${}^7\text{Be}$

Our ${}^7\text{Li}$ results with the TNI are summarized in Table III and Fig. 2. We show the basis size dependence up to $6\hbar\Omega$ using the optimal frequency $\hbar\Omega = 14$ MeV. We note that the $6\hbar\Omega$ ${}^7\text{Li}$ calculation is the most complex one among those presented in this paper. The three-body effective interaction basis space is defined by $N_{3\text{max}} = 9$ and there are

741 823 056 three-nucleon M -scheme matrix elements that we input in the shell model code. Although the dimension of the Hamiltonian matrix is only 663 527, it is significantly less sparse when a three-body interaction is present, e.g., there are 4 555 058 857 non-zero matrix elements compared to 235 927 305 for a calculations with just a two-body interaction.

From our ${}^7\text{Li}$ results we can draw similar conclusions as from the ${}^6\text{Li}$ results. A particularly important observation is the excitation energy convergence pattern, i.e., good stability of the spectra when increasing the basis size from $4\hbar\Omega$ to $6\hbar\Omega$ for both calculations with the TNI and without the TNI. There is an expected increase of binding energy and sensitivity of the spectra to the presence of the TNI. The level ordering is unchanged for the 9 levels that we show. Note that when compared to the old experimental evaluation of Ref. [21] we obtain the reversed order of $\frac{3}{2}^- \frac{1}{2}$ and $\frac{7}{2}^- \frac{1}{2}$ states, consistently with previous NCSM studies, e.g., [26]. However, the new evaluation [22] changes the order and energies of the two levels and, in addition, adds a new $\frac{1}{2}^- \frac{1}{2}$ level. Our calculated level ordering then matches the new evaluated level ordering. Note that our calculation with the TNI shows a slightly improved relative level spacing for those three levels compared to experiment. Similarly, the relative level spacing of the $\frac{7}{2}^- \frac{1}{2}$, $\frac{5}{2}^- \frac{1}{2}$ and $\frac{5}{2}^- \frac{1}{2}$ states is improved compared to experiment in the calculation with the TNI. Also we note that the lowest two excited states, $\frac{1}{2}^- \frac{1}{2}$ and $\frac{7}{2}^- \frac{1}{2}$, move closer to experiment when the TNI is present.

In Table III, we also show our results for ${}^7\text{Be}$ and, in particular, the Gamow-Teller transitions from the ${}^7\text{Be}$ ground state to the ground state and the first excited state of ${}^7\text{Li}$. There is a slight overall improvement when the TNI is included. The same transitions were calculated by Schiavilla and Wiringa using the the AV18/Urbana-IX interaction [24]. Our Gamow-Teller matrix element results compare well with theirs in particular for the ground-state to ground-state transition.

C. ${}^8\text{Be}$

We investigated ${}^8\text{Be}$ with an emphasis on the intruder states using two-nucleon interactions in Ref. [27] and also in Ref. [4]. Our ${}^8\text{Be}$ results with the TNI are summarized in Table IV and Fig. 3. We compare results obtained using three-body effective interaction derived from the AV8' two-nucleon interaction and from the AV8'+TM'(99) interaction, respectively, in the $4\hbar\Omega$ basis space using the optimal frequency $\hbar\Omega = 14$ MeV. It should be pointed out that our excitation spectra calculation without the TNI is actually in a very reasonable agreement with experiment. It is comforting that turning on the TM'(99) three-nucleon interaction does not really change the excitation spectrum very much and the quality of agreement with experiment is about the same. With the TNI we gain almost 4 MeV of binding energy. Also, we observe a stronger isospin mixing of the 2^+ and the 1^+ $T = 0, 1$ doublets. We note that in experiment, the 2^+ states at 16.6 and 16.9 MeV have strongly mixed $T = 0$ and $T = 1$ components. In Table IV, we present the intruder $0_2^+ 0$ state that was subject of our study in Ref. [27]. The position of this state, which is dominated by higher than $0\hbar\Omega$ components in the wave function, is strongly dependent on the basis size and still a much larger basis is needed for convergence. In Ref. [27], we investigated this state using basis spaces up to $10\hbar\Omega$, although employing just the two-body effective interaction. We note that the TNI affects this state by increasing its energy from 26.5 MeV by about 1 MeV in the $4\hbar\Omega$ space. However, this is not significant as we extrapolate the position of this state with the basis size increase to be in the 10-15 MeV range [27].

D. ${}^{10}\text{B}$, ${}^{10}\text{Be}$, ${}^{10}\text{C}$

Detailed $A = 10$ NCSM calculations using realistic two-nucleon interactions were presented in Ref. [28]. In addition, we investigated ${}^{10}\text{B}$ using three-body effective interaction derived from the AV8' NN interaction in Ref. [4]. Our ${}^{10}\text{B}$ results obtained with the TNI are compared to the two-nucleon interaction calculation in Table V and Fig. 4. We present only experimental states known to be predominantly of p -shell character as discussed earlier. In ${}^{10}\text{B}$ there are sd -shell dominated low-lying states, $1^+ 0$ at 5.18 MeV and $0^+ 1$ at 7.56 MeV that we obtain at much higher excitation energies in the basis spaces employed in this investigation [28]. Note that in Fig. 4, the two-nucleon interaction excitation energy results are displayed relative to the $1_1^+ 0$ state while in Table V the same results are given relative to the $3_1^+ 0$ state. We note that our calculations with realistic two-nucleon interactions predict an incorrect ground-state spin in this nucleus [4, 28], i.e., $1_1^+ 0$ instead of the experimental $3_1^+ 0$. The same prediction is obtained by the GFMC method [9]. Therefore, it is particularly interesting and important to investigate this nucleus using a Hamiltonian that includes a realistic three-nucleon interaction. Our results obtained using the TM'(99) TNI indeed show that the three-nucleon interaction has a positive impact on the excitation spectrum and corrects the level ordering by bringing the $3_1^+ 0$ state below the $1_1^+ 0$ state in agreement with experiment. Level ordering improves also for other excited states. This is particularly apparent when we present the excitation energies relative to the $3_1^+ 0$ state as done

in Table V. In the GFMC calculations of Ref. [9], the correct ^{10}B ground state was obtained using the Illinois TNI but the 1_1^+0 ground state remained when the Urbana IX TNI was employed. Combined with our observed sensitivity for higher excited states this shows that nuclear structure will play an important role in determining the form and the parametrization of the three-nucleon interaction that, unlike the two-nucleon interaction, is still not well known. Concerning the binding energies, with the TM'(99) we gain almost 6 MeV for the 3_1^+0 state and about 4 MeV for the 1_1^+0 state.

Our ^{10}Be and ^{10}C results are presented also in Table V. In particular, we paid attention to the Gamow-Teller transitions from the ^{10}B ground state to the 2^+1 states of ^{10}Be and the transition from the ^{10}C ground state to the 1_1^+0 state of ^{10}B . Overall, we observe a clear improvement compared to experiment in calculations that include the TNI. In the excitation spectra, we note the increased splitting between the 2_1^+1 and the 2_2^+1 states when TNI is included, again an improvement compared to experiment.

E. ^{11}B , ^{11}C

There were no published NCSM calculations for ^{11}B up to now. Our ^{11}B results with and without the TNI are summarized in Table VI and Fig. 5. We compare results obtained using three-body effective interaction derived from the AV8' two-nucleon interaction and from the AV8'+TM'(99) interaction, respectively, in the $4\hbar\Omega$ basis space using the same optimal frequency as for ^{10}B , i.e., $\hbar\Omega = 15$ MeV. All shown calculated states are $0\hbar\Omega$ dominated. It is not straightforward to make a correct correspondence to the experimental $T = \frac{1}{2}$ levels in particular above 10 MeV of excitation energy. We follow Refs. [33, 34] in making assignments in Table VI and Fig. 5. The $T = \frac{3}{2}$ level energies are taken from Refs. [32, 35]. Similarly as for ^{10}B , in Fig. 5, the two-nucleon interaction excitation energy results are displayed relative to the $\frac{1}{2}_1^-\frac{1}{2}$ state while in Table VI the same results are given relative to the $\frac{3}{2}_1^-\frac{1}{2}$ state. Given the complicated situation in neighboring ^{10}B , it is quite interesting to investigate ^{11}B . Although we have not done a detailed frequency dependence study as for ^{10}B , our present calculation suggest that the AV8' NN potential by itself might produce the incorrect ground state $\frac{1}{2}_1^-\frac{1}{2}$ instead of the experimentally observed $\frac{3}{2}_1^-\frac{1}{2}$ state. More calculations are needed to explore this issue but based on our present calculations we can definitely expect that a realistic two-nucleon interaction will predict the $\frac{3}{2}_1^-$ and $\frac{1}{2}_1^-$ states almost degenerate. In our $4\hbar\Omega$ calculation with the AV8' we obtain an incorrect ground state spin for ^{11}B . By including the TM'(99) this is corrected together with the level ordering of $\frac{5}{2}_1^-\frac{1}{2}$ and $\frac{3}{2}_2^-\frac{1}{2}$ states. In addition, the level spacing improves for majority of the low-lying states shown in Fig. 5 and Table VI. The binding energy gain is about 6 MeV.

As for ^{11}B , the calculation with the TNI produces a superior excitation spectrum and the correct ground-state spin for ^{11}C . An exception where there is a shift away from experiment in the calculations with the TNI appears for the ground-state magnetic moments of ^{11}B and ^{11}C . Recently, the Gamow-Teller transition strength for the $^{11}\text{B} \rightarrow ^{11}\text{C}$ was measured from the $^{11}\text{B}(p,n)^{11}\text{C}$ reaction [31]. In Table VI, we summarize the experimental and our calculated Gamow-Teller transition results. Overall, much better agreement is obtained in the calculation with the TNI.

F. ^{12}C , ^{12}B , ^{12}N

Detailed ^{12}C NCSM calculations using realistic two-nucleon interactions were reported in Ref. [1]. Here we extend those calculations by including the TNI. In Table VII, we summarize some of our results. In Fig. 6, we compare the excitation energies obtained with and without the TNI. In addition to an increase of binding energy by 6 MeV, we observe a sensitivity of the low-lying spectra to the presence of the realistic three-body force and a trend toward level-ordering improvement in comparison to experiment. The sensitivity is the largest for states where the spin-orbit interaction strength is known to play a role. Note the correct ordering of the $1^+0 \leftrightarrow 4^+0$ states and ordering and spacing improvement of the lowest $T=1$ states. In fact, the lowest $T = 1$ state, the isospin analog state of the ^{12}N and ^{12}B ground state comes out wrong, i.e., 0_1^+1 instead of 1_1^+1 , in the calculation with just the AV8'. Once the TM'(99) is included we obtain the correct 1_1^+1 state as the lowest $T = 1$ state and, moreover, the correct ordering of the next two lowest $T = 1$ states, 2_1^+1 and 0_1^+1 .

We note that in Fig. 6 we also show low-lying ^{12}C states that are dominated by higher than p -shell configurations. We obtain such states at much higher excitation energies in the basis spaces employed in this investigation.

The NCSM calculated binding energy of ^{12}C decreases with the basis size enlargement [1]. We extrapolate the binding energy for the AV8' NN potential to be less than 80 MeV. Consequently, we expect the binding energy for the AV8'+TM'(99) also decrease if we were able to reach the $6\hbar\Omega$ or larger basis space. Therefore, the good agreement of the AV8'+TM'(99) binding energy in the $4\hbar\Omega$ space with experiment shown in Table VII could be accidental. To

have a better insight on this issue, we need to perform more calculations, i.e., frequency and basis size dependence.

It is well known that the isovector $M1$ transition from the ^{12}C ground state to the 15.11 MeV 1_1^+1 state is very sensitive to the strength of the spin orbit interaction. Our $B(M1; 0^+0 \rightarrow 1^+1)$ results are presented in Fig. 7. The calculations with the 2-nucleon interaction show saturation and under-predict the experiment by almost a factor of three. By including the three-nucleon interaction, the $B(M1)$ value increases dramatically. This improvement is almost entirely due to the improved strength of the spin-orbit splitting when the three-nucleon interaction is included. The basis size dependence is stronger in this case. Clearly, if we were able to extend our calculations to the $6\hbar\Omega$ space, we would get much closer to the $B(M1)$ experimental value. We also note a substantial increase and overall better agreement with experiment for the $B(E2; 2_1^+1 \rightarrow 0_1^+0)$ in the calculation with the TNI (see Table VII).

Our results for ^{12}N and ^{12}B presented in Table VII further support the above discussed observations. In particular, the correct ground-state spin is obtained only in calculations that include the TNI. There is a significant improvement in level spacing even for the higher excited state, e.g., $2_2^+1, 1_2^+1$ and 3_1^+1 . It is interesting to note the complicated situation concerning the magnetic moments of the ^{12}N and ^{12}B ground states. In the calculation, there is a significant cancellation between orbital and spin contributions and, in particular, between proton and neutron spin contributions. Clearly, the calculations with the TNI improve agreement with experiment, although a significant discrepancy remains. The Gamow-Teller ground-state to ground-state transitions behave as the $M1$ isovector transition from the ^{12}C ground state to the 15.11 MeV 1_1^+1 state. The improvement compared to experiment is quite dramatic when the TNI is included.

G. ^{13}C

NCSM calculations for ^{13}C using a two-nucleon interaction were reported in Ref. [36]. In that work, the NCSM one-body transition densities were used for the DWBA description of proton and ^3He scattering on ^{13}C . Our present ^{13}C results obtained with and without the TNI are compared in Table IX and Fig. 8. We used the $4\hbar\Omega$ basis space using the same optimal frequency as for ^{12}C , i.e., $\hbar\Omega = 15$ MeV. The excitation spectrum of ^{13}C is quite complex. As we discussed earlier our calculated states presented in this study are all $0\hbar\Omega$ dominated. It is important to make a correct correspondence to the experimental levels as it is to be expected that the sd -shell dominated states would appear at low energies in ^{13}C . The character of low-lying ^{13}C states was studied in Ref. [37]. We use assignments found in Ref. [37] in our Table IX and Fig. 8. Despite the complexity of the ^{13}C excitation spectra the NCSM calculation obtains the lowest six states in correct order in both calculations with and without the TNI. When the TNI is included the lowest five states excitation energies improve compared to experiment. Note in particular an increase of the excitation energy of the $\frac{3}{2}_1^- \frac{1}{2}$ state. Also, the position of the lowest $T = \frac{3}{2}$ state $\frac{3}{2}_1^- \frac{3}{2}$ improves. From Table IX we can see that our $\text{AV8}' + \text{TM}'(99)$ $4\hbar\Omega$ calculation slightly overbinds ^{13}C . Similar comment as in Subsection III F on ^{12}C applies. We expect the binding energy decrease with the basis enlargement.

IV. EFFECTS OF THE THREE-NUCLEON INTERACTION

Overall, we find that three-nucleon interactions, and in particular the $\text{TM}'(99)$ force employed in this work, do have an important effect on nuclear structure. Of course, the primary expectation from previous studies of three- and four-nucleon systems with exact methods, is that the TNI will provide more binding energy in many-body systems. This requirement was certainly verified with previous NCSM and GFMC studies using realistic NN interactions. This is also borne out in the tables, and in the discussion that follows we focus primarily on the $A \leq 10$ nuclei, where the results with just the NN-interaction are reasonably converged, and are likely to be within 1 MeV of the exact results [4]. For ^6Li , the NN-interaction accounts for nearly 89% of the binding energy, while for ^7Li , ^8Be , and ^{10}B it accounts for 84-86% of the total binding. The $\text{TM}'(99)$ force then contributes an additional binding of the order 8-10% of the value obtained from the NN-interaction alone. What is somewhat remarkable is that the results with the TNI in ^6Li come quite close to the experimental binding energy (underbinding by less than 1 MeV), while the TNI significantly underbinds the $A \geq 7$ nuclei by 3.5-4.2 MeV. It is interesting that the underbinding becomes more dramatic with the addition just a single nucleon, i.e., from ^6Li to ^7Li . The nature of the underbinding requires further research. We plan to address three avenues of investigation. The first is the effects of the smaller three-particle model space on the convergence of the three-body effective interaction, which may be more severe for smaller oscillator frequencies. Although, our expectation is that the full effect of the underbinding is not due to a convergence issue. Efforts to upgrade the computer programs used to evaluate $V_{\text{3eff},123}^{\text{NN+NNN}}$ to use larger three-particle model spaces are underway. Second, we are also in the process of improving our shell-model codes to extend the calculations up to $N_{\text{max}} = 8$ for $A = 6, 7$ and $N_{\text{max}} = 6$ for $8 \leq A \leq 16$ nuclei. This extension is important in order to be able to fully

assess the effect of the TNI on the structure of $6 \leq A \leq 10$ nuclei. Finally, with these new capabilities, we hope to turn to the form of the TNI itself, which is not yet fully determined.

The other important feature of the TNI is the enhancement of spin-orbit effects. This is particularly evident in ^{10}B , where the inversion of the 1^+0 and 3^+0 states is a clear indication that the NN-interaction by itself is insufficient. A similar ground-state level inversions are observed for ^{11}B , and ^{12}N , ^{12}B . It is to be noted that the correct ordering is obtained with a realistic TNI with no free parameters (other than a cutoff fixed by reproducing the $A = 3$ binding energies). In addition, several calculated Gamow-Teller and $M1$ transitions are in better agreement with experiment when the TNI is included. These results are promising in that the inclusion of the TNI can improve our overall picture of the structure of light nuclei.

V. CONCLUSIONS

We extended the *ab initio* no-core shell model to include a realistic three-body interaction in calculations for p -shell nuclei. We presented results of first applications to $^{6,7}\text{Li}$, ^6He , ^8Be , $^{10,11,12}\text{B}$, ^{12}N and $^{10,12,13}\text{C}$ using the Argonne V8' NN potential and the chiral-symmetry-based Tucson-Melbourne TM'(99) three-nucleon interaction. In general, in addition to increase of binding energy, we observed a substantial sensitivity of the low-lying spectra to the presence of the realistic three-nucleon interaction and a trend toward level-ordering and level-spacing improvement in comparison to experiment. The sensitivity is the largest for states where the spin-orbit interaction strength is known to play a role. In particular, with the TNI we obtain the correct ground-state spin for $^{10,11}\text{B}$ and ^{12}N , ^{12}B , contrary to calculations with NN potentials only. In addition, we observe an overall improvement of the Gamow-Teller transition description in calculations with the three-nucleon interaction. The most striking case appears in $A = 12$ nuclei for the $0_1^+0 \rightarrow 1_1^+1$ transitions.

Unlike two-nucleon interaction, a detailed form and parametrization of the TNI is not well established yet, and it is highly likely that the sensitivity of the excitation spectra to the presence of the three-nucleon interaction could be exploited in determining the structure of the three-nucleon interaction itself. This is a topic that we plan to pursue in the future.

Until now calculations with a realistic TNI in the p -shell has been performed only using the GFMC method [6, 7, 8, 9] and by the coupled cluster method for ^{16}O [39]. Our NCSM approach has some advantages compared to those methods such as access to wider range of nuclei and also obtaining a more complete set of excited states. An important issue for the NCSM is the convergence which implies the need to use as large basis space as possible. With some algorithm and coding developments it should be feasible to perform $8\hbar\Omega$ calculations with the TNI for the light p -shell nuclei and $6\hbar\Omega$ calculations for the rest of the p -shell in a near future. Another important topic is the use of a greater variety of three-nucleon interactions and their different parametrizations including implementation of additional terms [19, 40] as well as the new effective field theory interactions developed in Ref. [41] and applied in Ref. [42]. A closely related issue is an improvement of efficiency and accuracy of the three-nucleon system solution calculations needed to construct the effective interaction as described in step (i) of Section II. A work in this direction is now under way [43].

VI. ACKNOWLEDGMENTS

We thank S. A. Coon, A. Nogga and D. J. Millener for useful comments. This work was performed under the auspices of the U. S. Department of Energy by the University of California, Lawrence Livermore National Laboratory under contract No. W-7405-Eng-48.

-
- [1] P. Navrátil, J. P. Vary and B. R. Barrett, Phys. Rev. Lett. **84**, 5728 (2000); Phys. Rev. C **62**, 054311 (2000).
 - [2] P. Navrátil and B. R. Barrett, Phys. Rev. C **59**, 1906 (1999).
 - [3] P. Navrátil, G. P. Kamuntavičius and B. R. Barrett, Phys. Rev. C **61**, 044001 (2000).
 - [4] P. Navrátil and W. E. Ormand, Phys. Rev. Lett. **88**, 152502 (2002).
 - [5] D. C. J. Marsden, P. Navrátil, S. A. Coon and B. R. Barrett, Phys. Rev. C **66**, 044007 (2002).
 - [6] B. S. Pudliner, V. R. Pandharipande, J. Carlson, S. C. Pieper and R. B. Wiringa, Phys. Rev. C **56**, 1720 (1997).
 - [7] R. B. Wiringa, S. C. Pieper, J. Carlson, V. R. Pandharipande, Phys. Rev. C **62**, 014001 (2000).
 - [8] S. C. Pieper, V. R. Pandharipande, R. B. Wiringa and J. Carlson, Phys. Rev. C **64**, 014001 (2001); S. C. Pieper and R. B. Wiringa, Ann. Rev. Nucl. Part. Sci. **51**, 53 (2001).

	$\mu a'$	$\mu^3 b$	$\mu^3 d$	Λ [μ]	g^2	μ [MeV]
TM'(99)	-1.12	-2.80	-0.72	4.7	172.1	138.0

TABLE I: Constants of the TM'(99) three-body force used in the present investigation.

- [9] S. C. Pieper, K. Varga and R. B. Wiringa, Phys. Rev. C **66**, 044310 (2002); R. B. Wiringa and S. C. Pieper, Phys. Rev. Lett. **89**, 182501 (2002).
- [10] S. A. Coon and H. K. Han, Few-Body Systems **30**, 131 (2001).
- [11] K. Suzuki and S. Y. Lee, Prog. Theor. Phys. **64**, 2091 (1980).
- [12] K. Suzuki, Prog. Theor. Phys. **68**, 246 (1982).
- [13] K. Suzuki and R. Okamoto, Prog. Theor. Phys. **70**, 439 (1983).
- [14] K. Suzuki and R. Okamoto, Prog. Theor. Phys. **92**, 1045 (1994).
- [15] L. Trlifaj, Phys. Rev. C **5**(5), 1534 (1972).
- [16] J. P. Vary, "The Many-Fermion-Dynamics Shell-Model Code", Iowa State University (1992) (unpublished).
- [17] W. E. Ormand and C. Johnson, private communication.
- [18] S. A. Coon, M. D. Scadron, P. C. McNamee, B. R. Barrett, D. W. E. Blatt and B. H. J. McKellar, Nucl. Phys. A **317**, 242 (1979).
- [19] J. L. Friar, D. Hüber, and U. van Kolck, Phys. Rev. C **59**, 53 (1999).
- [20] P. Navrátil, J. P. Vary, W. E. Ormand and B. R. Barrett, Phys. Rev. Lett. **87**, 172502 (2001).
- [21] F. Ajzenberg-Selove, Nucl. Phys. A **490**, 1 (1988).
- [22] D. R. Tilley, C. M. Cheves, J. L. Godwin, G. M. Hale, H. M. Hofmann, J. H. Kelley, C. G. Sheu and H. R. Weller, Nucl. Phys. A **708**, 3 (2002).
- [23] I. Tanihata, T. Kobayashi, O. Yamakawa, S. Shimoura, K. Ekuni, K. Sugimoto, N. Takahashi, T. Shimoda and H. Sato, Phys. Lett. B **206**, 592 (1988); A. Ozawa, I. Tanihata, T. Kobayashi, Y. Sugahara, O. Yamakawa, K. Omata, K. Sugimoto, D. Olson, W. Christie and H. Wieman, Nucl. Phys. A **608**, 63 (1996); H. De Vries, C. W. De Jager and C. De Vries, At. Data Nucl. Data Tab. **36**, 495 (1987).
- [24] R. Schiavilla and R. B. Wiringa, Phys. Rev. C **65**, 054302 (2002).
- [25] W.-T. Chou, E. K. Warburton and B. A. Brown, Phys. Rev. C **47**, 163 (1993).
- [26] P. Navrátil and B. R. Barrett, Phys. Rev. C **57**, 3119 (1998).
- [27] E. Caurier, P. Navrátil, W. E. Ormand and J. P. Vary, Phys. Rev. C **64**, 051301 (2001).
- [28] E. Caurier, P. Navrátil, W. E. Ormand and J. P. Vary, Phys. Rev. C **66**, 024314 (2002).
- [29] I. Daito *et al.*, Phys. Lett. B **418**, 27 (1998).
- [30] F. Ajzenberg-Selove, Nucl. Phys. A **506**, 1 (1990).
- [31] T. N. Taddeucci *et al.*, Phys. Rev. C **42**, 935 (1990).
- [32] R. Aryaeinejad *et al.*, Nucl. Phys. A **436**, 1 (1985).
- [33] A. A. Wolters, A. G. M. van Hees and P. W. M. Glaudemans, Phys. Rev. C **42**, 2062 (1990).
- [34] D. J. Millener, private communication.
- [35] D. J. Millener, Nucl. Phys. A **693**, 394 (2001).
- [36] G. Thiamová, V. Burjan, J. Cejpek, V. Kroha and P. Navrátil, Nucl. Phys. A **697**, 25 (2002).
- [37] D. J. Millener, D. I. Sober, H. Crannell, J. T. O'Brien, L. W. Fagg, S. Kowalski, C. F. Williamson and L. Lapikás, Phys. Rev. C **39**, 14 (1989).
- [38] F. Ajzenberg-Selove, Nucl. Phys. A **523**, 1 (1991).
- [39] B. Mihaila and J. H. Heisenberg, Phys. Rev. C **61**, 054309 (2000).
- [40] S. A. Coon and J. L. Friar, Phys. Rev. C **34**, 34 (1986).
- [41] U. Van Kolck, Phys. Rev. C **49**, 2932 (1994).
- [42] E. Epelbaum, A. Nogga, W. Glöckle, H. Kamada, Ulf-G. Meissner and H. Witala, Phys. Rev. C **66**, 064001 (2002).
- [43] A. Nogga, private communication.

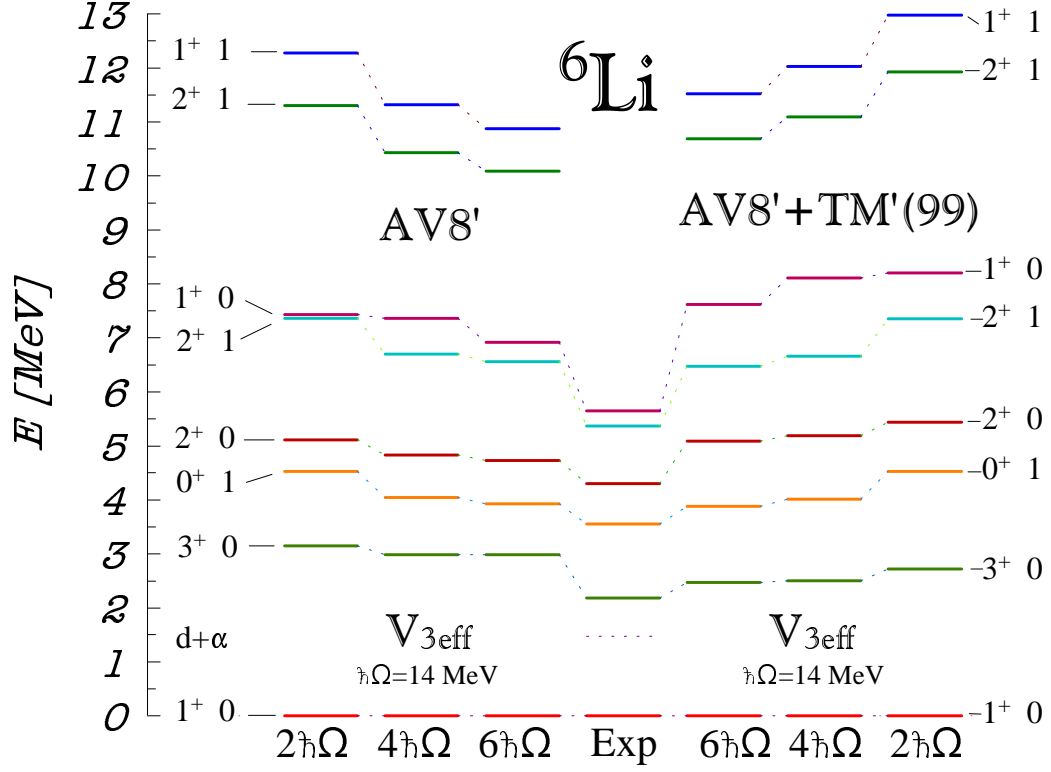


FIG. 1: Calculated positive-parity excitation spectra of ${}^6\text{Li}$ obtained in $2\hbar\Omega$ - $6\hbar\Omega$ basis spaces using three-body effective interactions derived from AV8' NN potential and AV8' NN potential plus TM'(99) three-nucleon interaction, respectively, are compared to experiment. The HO frequency of $\hbar\Omega = 14 \text{ MeV}$ was used. The experimental values are from Ref. [21].

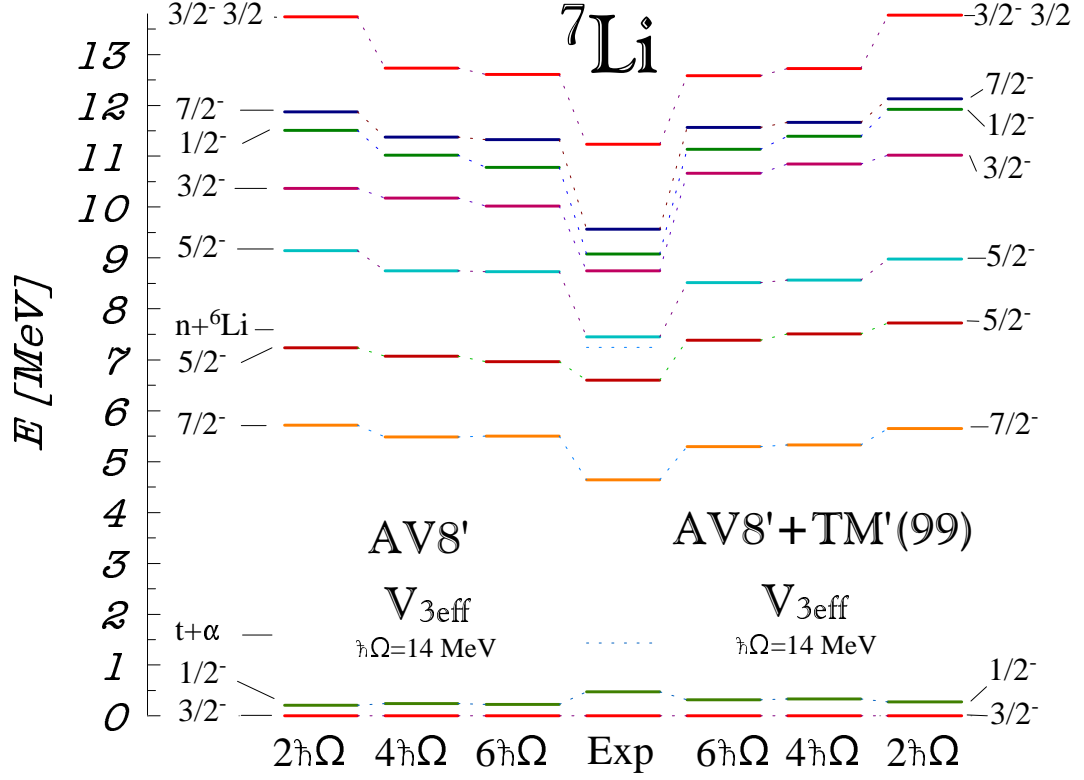


FIG. 2: Calculated negative-parity excitation spectra of ${}^7\text{Li}$ obtained in $2\hbar\Omega$ - $6\hbar\Omega$ basis spaces using three-body effective interactions derived from $\text{AV8}'$ NN potential and $\text{AV8}'$ NN potential plus $\text{TM}'(99)$ three-nucleon interaction, respectively, are compared to experiment. The HO frequency of $\hbar\Omega = 14 \text{ MeV}$ was used. The experimental values are from Ref. [22].

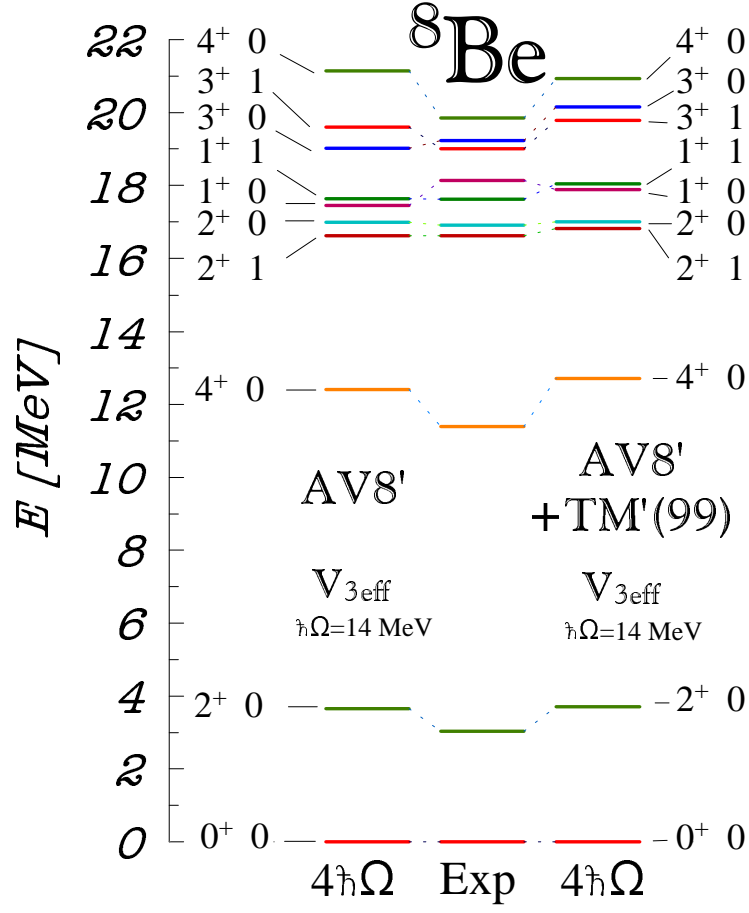


FIG. 3: Calculated positive-parity excitation spectra of ${}^8\text{Be}$ obtained in $4\hbar\Omega$ basis space using three-body effective interaction derived from AV8' NN potential and AV8' NN potential plus TM'(99) three-nucleon interaction, respectively, are compared to experiment. The HO frequency of $\hbar\Omega = 14 \text{ MeV}$ was used. The experimental values are from Ref. [21].

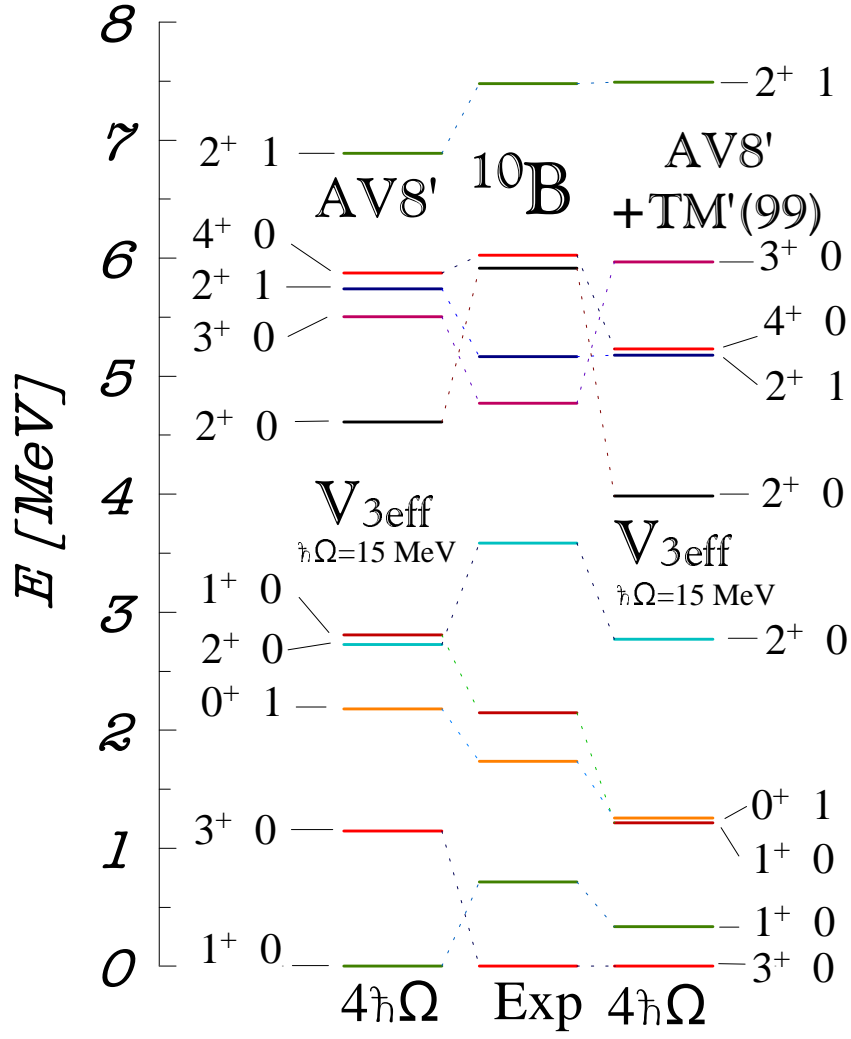


FIG. 4: Calculated positive-parity excitation spectra of ^{10}B obtained in $4\hbar\Omega$ basis space using three-body effective interaction derived from AV8' NN potential and AV8' NN potential plus TM'(99) three-nucleon interaction, respectively, are compared to experiment. The HO frequency of $\hbar\Omega = 15$ MeV was used. The experimental values are from Ref. [21].

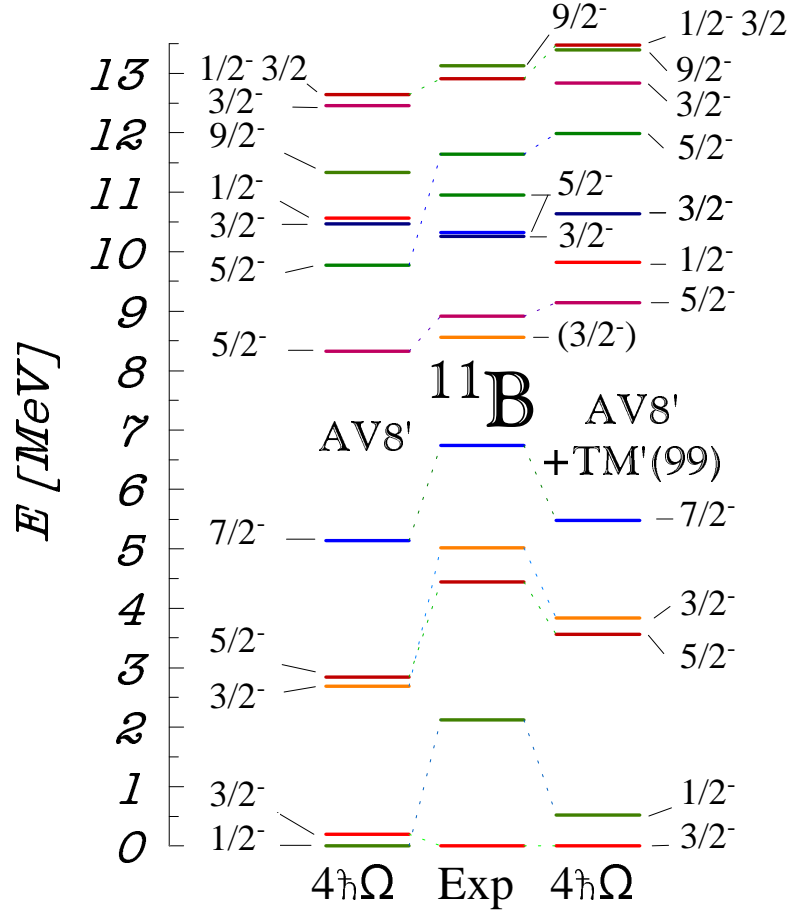


FIG. 5: Calculated negative-parity excitation spectra of ^{11}B obtained in $4\hbar\Omega$ basis space using three-body effective interaction derived from AV8' NN potential and AV8' NN potential plus TM'(99) three-nucleon interaction, respectively, are compared to experiment. The HO frequency of $\hbar\Omega = 15$ MeV was used. Assignments are made only to experimental states that are known to be dominantly of p -shell character. The experimental values are from Ref. [30, 32].

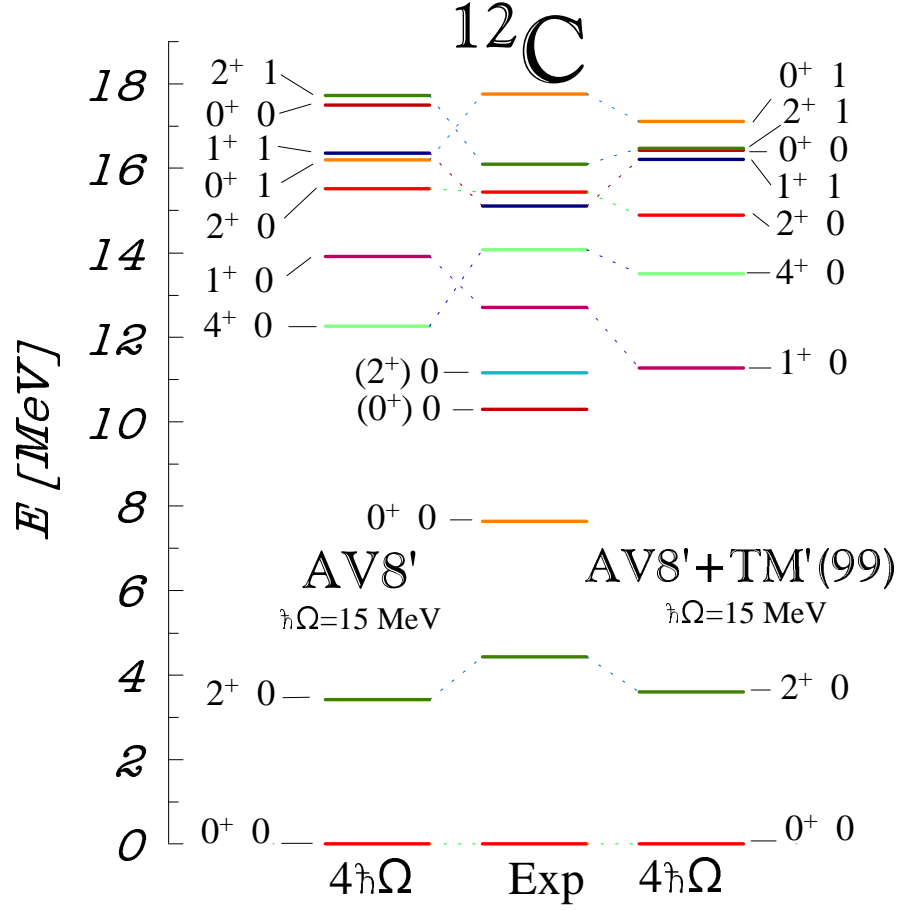


FIG. 6: Calculated positive-parity excitation spectra of ^{12}C obtained in $4\hbar\Omega$ basis space using three-body effective interaction derived from AV8' NN potential and AV8' NN potential plus TM'(99) three-nucleon interaction, respectively, are compared to experiment. The HO frequency of $\hbar\Omega = 15 \text{ MeV}$ was used. The experimental values are from Ref. [30].

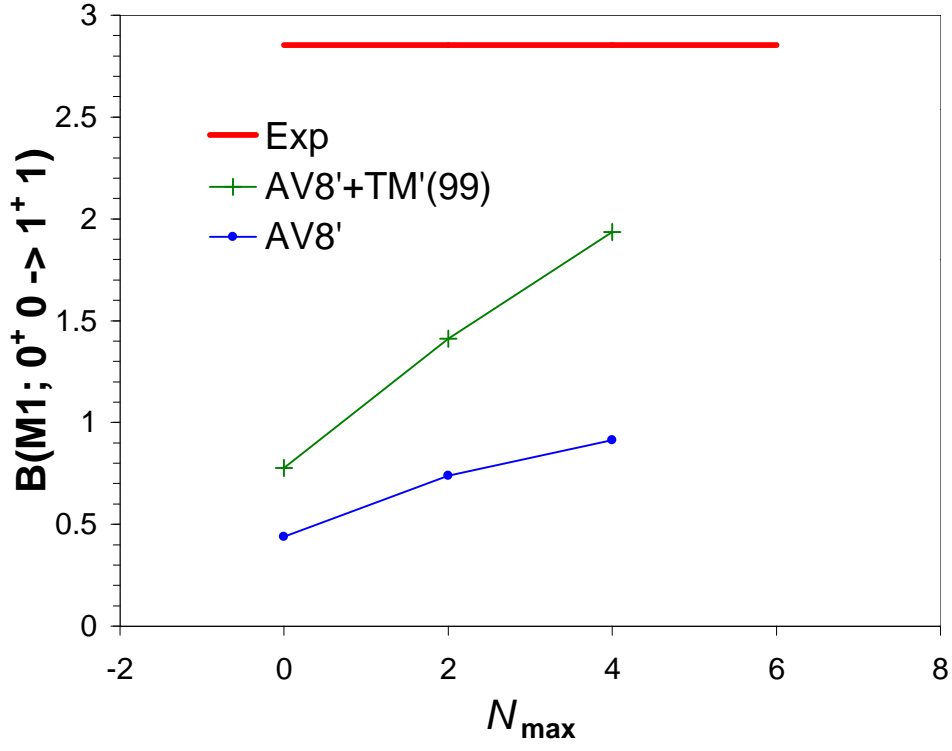


FIG. 7: Experimental and calculated $B(M1)$ values, in μ_N^2 , for the $0^+0 \rightarrow 1^+1$ transition in ^{12}C . Results obtained using the AV8' and AV8'+TM'(99) interactions in basis spaces up to $4\hbar\Omega$ are compared. The HO frequency of $\hbar\Omega = 15$ MeV was used. The experimental values are from Ref. [30].

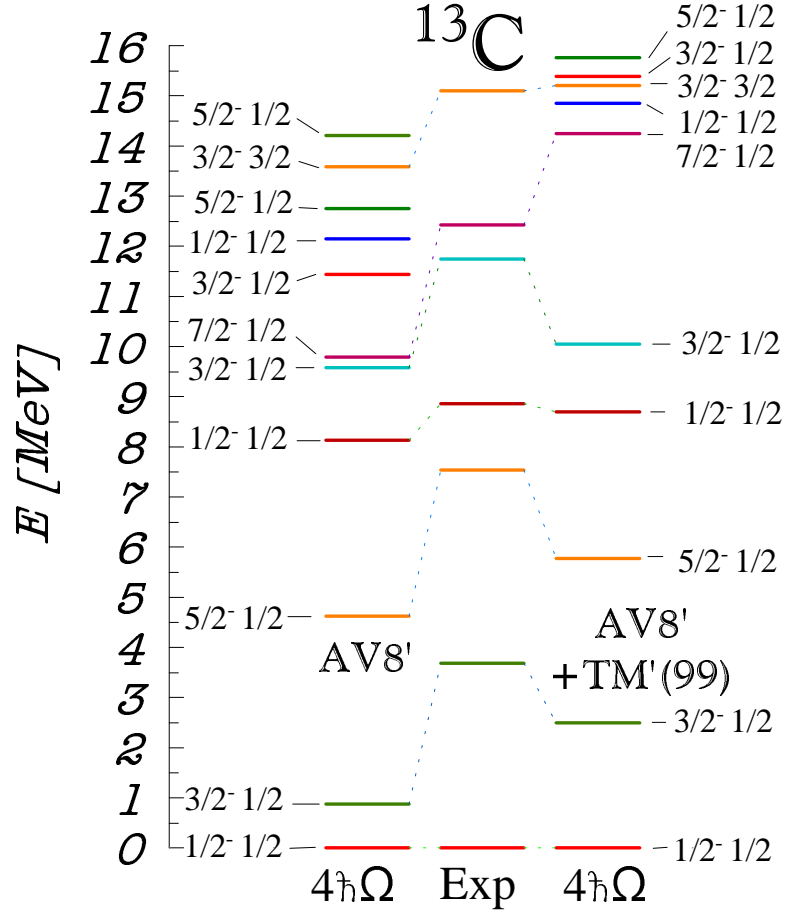


FIG. 8: Calculated negative-parity excitation spectra of ^{13}C obtained in $4\hbar\Omega$ basis space using three-body effective interaction derived from AV8' NN potential and AV8' NN potential plus TM'(99) three-nucleon interaction, respectively, are compared to experiment. The HO frequency of $\hbar\Omega = 15$ MeV was used. The level assignments are made according to Ref. [37]. Only experimental states known to be dominantly of p -shell character are shown. The experimental values are from Ref. [38].

⁶ Li	Exp	AV8'+TM'(99)	AV8'
basis space	-	6 $\hbar\Omega$	6 $\hbar\Omega$
$ E_{\text{gs}} (1^+0)$	31.995	31.036	28.406
r_p [fm]	2.32(3)	2.054	2.097
Q_{gs} [$e \text{ fm}^2$]	-0.082(2)	-0.025	-0.102
μ_{gs} [μ_N^2]	+0.822	+0.840	+0.848
$E_x(1_1^+0)$	0.0	0.0	0.0
$E_x(3^+0)$	2.186	2.471	2.986
$E_x(0^+1)$	3.563	3.886	3.933
$E_x(2^+0)$	4.312	5.010	4.733
$E_x(2_1^+1)$	5.366	6.482	6.563
$E_x(1_2^+0)$	5.65	7.621	6.922
$E_x(2_2^+1)$		10.693	10.095
$E_x(1^+1)$		11.525	10.881
B(E2; $1_1^+0 \rightarrow 3^+0$)	21.8(4.8)	7.093	8.412
B(M1; $0^+1 \rightarrow 1_1^+0$)	15.42(32)	15.374	15.234
B(E2; $2^+0 \rightarrow 1_1^+0$)	4.41(2.27)	3.129	3.491
B(M1; $2_1^+1 \rightarrow 1_1^+0$)	0.150(27)	0.113	0.027
⁶ He	Exp	AV8'+TM'(99)	AV8'
basis space	-	6 $\hbar\Omega$	6 $\hbar\Omega$
$ E_{\text{gs}} (0^+1)$	29.269	28.189	25.488
r_p [fm]	1.72(4)	1.707	1.743
$E_x(0_1^+1)$	0.0	0.0	0.0
$E_x(2^+1)$	1.8	2.598	2.638
$E_x(2^+1)$		6.892	6.231
$E_x(1^+1)$		7.737	7.035
$E_x(0_2^+1)$		10.855	9.467
⁶ He \rightarrow ⁶ Li	Exp	AV8'+TM'(99)	AV8'
basis space	-	6 $\hbar\Omega$	6 $\hbar\Omega$
B(GT; $0_1^+1 \rightarrow 1_1^+0$)	4.728(15)	5.213	5.314

TABLE II: Experimental and calculated energies, in MeV, ground-state point-proton rms radii, quadrupole and magnetic moments, as well as E2, in $e^2 \text{ fm}^4$, and M1, in μ_N^2 , transitions of ⁶Li and ⁶He as well as the B(GT) values for the ⁶He ground state to ⁶Li ground state transition. Results obtained using three-body effective interactions derived from the AV8' and AV8'+TM'(99) interactions are presented. A HO frequency of $\hbar\Omega = 14$ MeV was employed. The experimental values are from Ref. [21, 22, 23].

${}^7\text{Li}$	Exp	AV8'+TM'(99)	AV8'
basis space	-	$6\hbar\Omega$	$6\hbar\Omega$
$ E_{\text{gs}}(\frac{3}{2}^-\frac{1}{2}) $	39.270	35.832	32.953
r_p [fm]	2.27(2)	2.071	2.104
Q_{gs} [e fm ²]	-4.00(6)	-2.563	-2.679
μ_{gs} [μ_N^2]	+3.256	+3.025	+3.012
$E_x(\frac{3}{2}_1^-\frac{1}{2})$	0.0	0.0	0.0
$E_x(\frac{1}{2}_1^-\frac{1}{2})$	0.478	0.317	0.229
$E_x(\frac{7}{2}_1^-\frac{1}{2})$	4.65	5.301	5.499
$E_x(\frac{5}{2}_1^-\frac{1}{2})$	6.60	7.388	6.971
$E_x(\frac{5}{2}_2^-\frac{1}{2})$	7.45	8.527	8.732
$E_x(\frac{3}{2}_2^-\frac{1}{2})$	8.75	10.668	10.026
$E_x(\frac{1}{2}_2^-\frac{1}{2})$	9.09	11.145	10.793
$E_x(\frac{7}{2}_2^-\frac{1}{2})$	9.57	11.568	11.331
$E_x(\frac{3}{2}_1^-\frac{3}{2})$	11.24	12.583	12.613
${}^7\text{Be}$	Exp	AV8'+TM'(99)	AV8'
basis space	-	$6\hbar\Omega$	$6\hbar\Omega$
$ E_{\text{gs}}(\frac{3}{2}^-\frac{1}{2}) $	37.600	34.176	31.318
r_p [fm]	2.36(2)	2.225	2.262
Q_{gs} [e fm ²]		-4.305	-4.614
μ_{gs} [μ_N^2]	-1.398(15)	-1.153	-1.138
$E_x(\frac{3}{2}_1^-\frac{1}{2})$	0.0	0.0	0.0
$E_x(\frac{1}{2}_1^-\frac{1}{2})$	0.429	0.309	0.225
$E_x(\frac{7}{2}_1^-\frac{1}{2})$	4.57(5)	5.232	5.429
$E_x(\frac{5}{2}_1^-\frac{1}{2})$	6.73(10)	7.329	6.912
$E_x(\frac{5}{2}_2^-\frac{1}{2})$	7.21(6)	8.333	8.514
${}^7\text{Be} \rightarrow {}^7\text{Li}$	Exp	AV8'+TM'(99)	AV8'
basis space	-	$6\hbar\Omega$	$6\hbar\Omega$
$\text{B}(\text{GT}; \frac{3}{2}_1^-\frac{1}{2} \rightarrow \frac{3}{2}_1^-\frac{1}{2})$	1.300	1.401	1.445
$\text{B}(\text{GT}; \frac{3}{2}_1^-\frac{1}{2} \rightarrow \frac{1}{2}_1^-\frac{1}{2})$	1.122	1.214	1.231

TABLE III: Experimental and calculated energies, in MeV, ground-state point-proton rms radii, quadrupole and magnetic moments, of ${}^7\text{Li}$ and ${}^7\text{Be}$ as well as the B(GT) values for the ${}^7\text{Be}$ to ${}^7\text{Li}$ transitions. Results obtained using three-body effective interactions derived from the AV8' and AV8'+TM'(99) interactions are presented. A HO frequency of $\hbar\Omega = 14$ MeV was employed. The experimental values are from Ref. [22, 23, 25].

⁸ Be basis space	Exp -	AV8'+TM'(99) 4 $\hbar\Omega$	AV8' 4 $\hbar\Omega$
$ E_{\text{gs}} $	56.50	52.328	48.454
$E_x(0_1^+0)$	0.0	0.0	0.0
$E_x(2_1^+0)$	3.04	3.724	3.652
$E_x(4_1^+0)$	11.40	12.713	12.402
$E_x(2_1^+1)^a$	16.63 ^a	16.831 ^a	16.630
$E_x(2_2^+0)^a$	16.92 ^a	17.009 ^a	16.998
$E_x(1_1^+1)$	17.64	18.049	17.649
$E_x(1_1^+0)$	18.15	17.895	17.463
$E_x(3_1^+1)$	19.01	19.797	19.608
$E_x(3_1^+0)$	19.24	20.163	19.028
$E_x(0_1^+1)$		20.910	19.525
$E_x(4_2^+0)$	19.86	20.942	21.144
$E_x(0_2^+0)$		27.705	26.478
$E_x(0_1^+2)$	27.49	28.931	28.335

^aT=0 and T=1 components strongly mixed

TABLE IV: Experimental and calculated energies, in MeV, of ⁸Be. Results obtained using three-body effective interactions derived from the AV8' and AV8'+TM'(99) interactions are presented. A HO frequency of $\hbar\Omega = 14$ MeV was employed. The experimental values are from Ref. [21].

¹⁰ B	Exp	AV8'+TM'(99)	AV8'
basis space	-	4ħΩ	4ħΩ
E(3 ⁺ 0)	64.751	60.567	54.833
r _p (3 ⁺ 0) [fm]	2.30(12)	2.168	2.196
Q ₃₊₀ [e fm ²]	+8.472(56)	+5.682	+5.937
μ ₃₊₀ [μ _N ²]	+1.8006	+1.847	+1.857
E(1 ⁺ 0)	64.033	60.227	55.979
μ ₁₊₀ [μ _N ²]	+0.63(12)	+0.802	+0.843
E _x (3 ₁ ⁺ 0)	0.0	0.0	0.0
E _x (1 ₁ ⁺ 0)	0.718	0.340	-1.146
E _x (0 ₁ ⁺ 1)	1.740	1.259	1.039
E _x (1 ₂ ⁺ 0)	2.154	1.216	1.664
E _x (2 ₁ ⁺ 0)	3.587	2.775	1.579
E _x (3 ₂ ⁺ 0)	4.774	5.971	4.363
E _x (2 ₁ ⁺ 1)	5.164	5.182	4.553
E _x (2 ₂ ⁺ 0)	5.92	3.987	3.470
E _x (4 ₁ ⁺ 0)	6.025	5.229	4.732
E _x (2 ₂ ⁺ 1)	7.478	7.491	5.741
B(E2;1 ₁ ⁺ 0 → 3 ₁ ⁺ 0)	4.13(6)	1.959	3.568
B(E2;1 ₂ ⁺ 0 → 3 ₁ ⁺ 0)	1.71(26)	1.010	0.047
B(E2;1 ₂ ⁺ 0 → 1 ₁ ⁺ 0)	0.83(40)	3.384	2.311
B(E2;3 ₂ ⁺ 0 → 1 ₁ ⁺ 0)	20.5(26)	3.543	3.289
¹⁰ Be	Exp	AV8'+TM'(99)	AV8'
basis space	-	4ħΩ	4ħΩ
E _{gs}	64.977	61.387	55.840
r _p [fm]	2.24(8)	2.087	2.113
E _x (0 ₁ ⁺ 1)	0.0	0.0	0.0
E _x (2 ₁ ⁺ 1)	3.368	3.877	3.463
E _x (2 ₂ ⁺ 1)	5.958	6.241	4.706
E _x (1 ₁ ⁺ 1)		8.532	7.582
E _x (3 ₁ ⁺ 1)		9.856	8.190
E _x (2 ₃ ⁺ 1)	9.4	10.036	9.040
¹⁰ B → ¹⁰ Be	Exp	AV8'+TM'(99)	AV8'
basis space	-	4ħΩ	4ħΩ
B(GT;3 ₁ ⁺ 0 → 2 ₁ ⁺ 1)	0.08(3)	0.066	0.062
B(GT;3 ₁ ⁺ 0 → 2 ₂ ⁺ 1)	0.95(13)	1.291	1.554
¹⁰ C	AV8'+TM'(99)	Exp	AV8'
basis space	-	4ħΩ	4ħΩ
E _{gs}	60.321	56.626	51.141
r _p [fm]	2.31(3)	2.246	2.279
E _x (0 ₁ ⁺ 1)	0.0	0.0	0.0
E _x (2 ₁ ⁺ 1)	3.354	3.913	3.508
E _x (2 ₂ ⁺ 1)		6.133	4.612
E _x (1 ₁ ⁺ 1)		8.437	7.453
E _x (3 ₁ ⁺ 1)		9.773	8.145
E _x (2 ₃ ⁺ 1)		10.049	9.009
less ¹⁰ C → ¹⁰ B	Exp	AV8'+TM'(99)	AV8'
basis space	-	4ħΩ	4ħΩ
B(GT;0 ₁ ⁺ 1 → 1 ₁ ⁺ 0)	3.44	4.331	4.748

TABLE V: Experimental and calculated energies, in MeV, ground-state point-proton rms radii, the quadrupole moments, as well as E2, in e² fm⁴, transitions of ¹⁰B, ¹⁰Be and ¹⁰C as well as selected Gamow-Teller transitions. Results obtained using three-body effective interactions derived from the AV8' and AV8'+TM'(99) interactions are presented. A HO frequency of ħΩ = 15 MeV was employed. The experimental values are from Ref. [21, 23, 25, 29].

¹¹ B	Exp	AV8'+TM'(99)	AV8'
basis space	-	$4\hbar\Omega$	$4\hbar\Omega$
$ E(\frac{3}{2}_1^{-}\frac{1}{2}) $	76.205	73.338	67.214
$r_p(\frac{3}{2}_1^{-}\frac{1}{2})$ [fm]	2.24(12)	2.148	2.175
$Q(\frac{3}{2}_1^{-}\frac{1}{2})$ [e fm ²]	+4.065(26)	+2.920	+2.674
$\mu(\frac{3}{2}_1^{-}\frac{1}{2})$ [μ_N^2]	+2.689	+2.176	+2.708
$ E(\frac{1}{2}_1^{-}\frac{1}{2}) $	74.080	72.816	67.413
$\mu(\frac{1}{2}_1^{-}\frac{1}{2})$ [μ_N^2]		-0.435	-0.505
$E_x(\frac{3}{2}_1^{-}\frac{1}{2})$	0.0	0.0	0.0
$E_x(\frac{1}{2}_1^{-}\frac{1}{2})$	2.125	0.522	-0.198
$E_x(\frac{5}{2}_1^{-}\frac{1}{2})$	4.445	3.565	2.642
$E_x(\frac{3}{2}_2^{-}\frac{1}{2})$	5.020	3.840	2.492
$E_x(\frac{7}{2}_1^{-}\frac{1}{2})$	6.743	5.481	4.946
$E_x(\frac{5}{2}_2^{-}\frac{1}{2})$	8.92	9.141	8.130
$E_x(\frac{1}{2}_2^{-}\frac{1}{2})$		9.819	10.372
$E_x(\frac{3}{2}_3^{-}\frac{1}{2})$		10.643	10.280
$E_x(\frac{5}{2}_3^{-}\frac{1}{2})$	11.64	11.989	9.572
$E_x(\frac{3}{2}_4^{-}\frac{1}{2})$		12.839	12.264
$E_x(\frac{1}{2}_1^{-}\frac{3}{2})$	12.916	13.479	12.443
$E_x(\frac{9}{2}_1^{-}\frac{1}{2})$		13.402	11.139
$E_x(\frac{7}{2}_2^{-}\frac{1}{2})$		14.026	12.143
$E_x(\frac{3}{2}_1^{-}\frac{3}{2})$	15.29	16.588	14.735
$E_x(\frac{5}{2}_1^{-}\frac{3}{2})$	16.50	17.056	15.968
B(E2; $\frac{3}{2}_1^{-}\frac{1}{2} \rightarrow \frac{1}{2}_1^{-}\frac{1}{2}$)	2.6(4)	1.141	0.522
¹¹ C	Exp	AV8'+TM'(99)	AV8'
basis space	-	$4\hbar\Omega$	$4\hbar\Omega$
$ E(\frac{3}{2}_1^{-}\frac{1}{2}) $	73.440	70.618	64.515
$Q(\frac{3}{2}_1^{-}\frac{1}{2})$ [e fm ²]	+3.327(24)	+2.363	+1.627
$\mu(\frac{3}{2}_1^{-}\frac{1}{2})$ [μ_N^2]	-0.964(1)	-0.460	-0.923
$ E(\frac{1}{2}_1^{-}\frac{1}{2}) $	71.440	70.093	64.712
$\mu(\frac{1}{2}_1^{-}\frac{1}{2})$ [μ_N^2]		+0.809	+0.882
$E_x(\frac{3}{2}_1^{-}\frac{1}{2})$	0.0	0.0	0.0
$E_x(\frac{1}{2}_1^{-}\frac{1}{2})$	2.000	0.525	-0.197
$E_x(\frac{5}{2}_1^{-}\frac{1}{2})$	4.319	3.584	2.656
$E_x(\frac{3}{2}_2^{-}\frac{1}{2})$	4.804	3.852	2.498
$E_x(\frac{7}{2}_1^{-}\frac{1}{2})$	6.478	5.363	4.848
$E_x(\frac{5}{2}_2^{-}\frac{1}{2})$	8.420	8.943	7.978
¹¹ B \rightarrow ¹¹ C	Exp	AV8'+TM'(99)	AV8'
basis space	-	$4\hbar\Omega$	$4\hbar\Omega$
B(GT; $\frac{3}{2}_1^{-}\frac{1}{2} \rightarrow \frac{3}{2}_1^{-}\frac{1}{2}$)	0.345	0.315	0.765
B(GT; $\frac{3}{2}_1^{-}\frac{1}{2} \rightarrow \frac{1}{2}_1^{-}\frac{1}{2}$)	0.399	0.591	0.909
B(GT; $\frac{3}{2}_1^{-}\frac{1}{2} \rightarrow \frac{5}{2}_1^{-}\frac{1}{2}$)	0.961 ^a	0.517	0.353
B(GT; $\frac{3}{2}_1^{-}\frac{1}{2} \rightarrow \frac{3}{2}_2^{-}\frac{1}{2}$)	0.961 ^a	0.741	0.531
B(GT; $\frac{3}{2}_1^{-}\frac{1}{2} \rightarrow \frac{5}{2}_2^{-}\frac{1}{2}$)	0.444 ^b	0.625	0.197

^aUnresolved doublet, $E_x = 4.32 + 4.80$ MeV, approximately equal strength.

^bUnresolved doublet, $E_x = 8.10 + 8.42$ MeV, most strength in the 8.42-MeV transition.

TABLE VI: Experimental and calculated energies, in MeV, ground-state point-proton rms radii, quadrupole and magnetic moments, E2, in e^2 fm⁴, transitions of ¹¹B and ¹¹C as well as the B(GT) values for the ¹¹B to ¹¹C transitions. Results obtained using three-body effective interactions derived from the AV8' and AV8'+TM'(99) interactions are presented. A HO frequency of $\hbar\Omega = 15$ MeV was employed. Only experimental states known to be dominantly of p -shell character are shown. The experimental values are from Ref. [23, 30, 31, 32].

^{12}C basis space	Exp -	AV8'+TM'(99) $4\hbar\Omega$	AV8' $4\hbar\Omega$
$ E_{\text{gs}} $	92.162	91.963	85.945
r_p [fm]	2.35(2)	2.191	2.209
Q_{2^+} [$e \text{ fm}^2$]	+6(3)	4.288	4.613
$E_x(0^+0)$	0.0	0.0	0.0
$E_x(2^+0)$	4.439	3.603	3.427
$E_x(1^+0)$	12.710	11.280	13.926
$E_x(4^+0)$	14.083	13.517	12.272
$E_x(1^+1)$	15.110	16.221	16.364
$E_x(2^+1)$	16.106	16.467	17.712
$E_x(0^+1)$	17.760	17.116	16.213
B(E2; $2^+0 \rightarrow 0^+0$)	7.59(42)	4.146	4.765
B(M1; $1^+1 \rightarrow 0^+0$)	0.951(20)	0.645	0.305
B(E2; $2^+1 \rightarrow 0^+0$)	0.65(13)	0.430	0.247

TABLE VII: Experimental and calculated energies, in MeV, the 2^+_1 -state quadrupole moments, as well as E2, in $e^2 \text{ fm}^4$, and M1, in μ_N^2 , transitions of ^{12}C . Results obtained using three-body effective interactions derived from the AV8' and AV8'+TM'(99) interactions are presented. A HO frequency of $\hbar\Omega = 15$ MeV was employed. The experimental values are from Ref. [23, 30].

^{12}B	Exp	AV8'+TM'(99)	AV8'
basis space	-	$4\hbar\Omega$	$4\hbar\Omega$
$ E(1_1^+1) $	79.578	78.379	72.209
$Q_{1_1^+1}$ [$e \text{ fm}^2$]	1.34(14)	+0.692	+0.772
$\mu_{1_1^+1}$ [μ_N^2]	+1.003	+0.2917	-0.130
$E_x(1_1^+1)$	0.0	0.0	0.0
$E_x(2_1^+1)$	0.953	0.216	1.335
$E_x(0_1^+1)$	2.723	0.854	-0.158
$E_x(2_2^+1)$	3.759(6)	3.124	1.533
$E_x(1_2^+1)$	5.00(20)	4.381	2.727
$E_x(3_1^+1)$	5.612(8)	5.205	3.630
$^{12}\text{C} \rightarrow ^{12}\text{B}$	Exp	AV8'+TM'(99)	AV8'
basis space	-	$4\hbar\Omega$	$4\hbar\Omega$
B(GT; $0_1^+0 \rightarrow 1_1^+1$)	0.990(2)	0.666	0.255
^{12}N	Exp	AV8'+TM'(99)	AV8'
basis space	-	$4\hbar\Omega$	$4\hbar\Omega$
$ E(1_1^+1) $	74.041	72.601	66.466
$Q_{1_1^+1}$ [$e \text{ fm}^2$]	+1.03(7)	+0.390	+0.386
$\mu_{1_1^+1}$ [μ_N^2]	+0.457	+1.124	+1.513
$E_x(1_1^+1)$	0.0	0.0	0.0
$E_x(2_1^+1)$	0.960(12)	0.236	1.338
$E_x(0_1^+1)$	2.439(9)	0.825	-0.167
$E_x(2_2^+1)$		3.104	1.534
$E_x(1_2^+1)$		4.392	2.733
$E_x(3_1^+1)$		5.077	3.547
$^{12}\text{C} \rightarrow ^{12}\text{N}$	Exp	AV8'+TM'(99)	AV8'
basis space	-	$4\hbar\Omega$	$4\hbar\Omega$
B(GT; $0_1^+0 \rightarrow 1_1^+1$)	0.877(3)	0.662	0.254

TABLE VIII: Experimental and calculated energies, in MeV, quadrupole and magnetic moments of ^{12}B and ^{12}N as well as the B(GT) values for the ^{12}C ground state to ^{12}B and ^{12}N ground state transition. Results obtained using three-body effective interactions derived from the AV8' and AV8'+TM'(99) interactions are presented. A HO frequency of $\hbar\Omega = 15$ MeV was employed. The experimental values are from Ref. [25, 30].

^{13}C basis space	Exp -	AV8'+TM'(99) $4\hbar\Omega$	AV8' $4\hbar\Omega$
$ E_{\text{gs}} $	97.108	99.220	91.889
r_p [fm]	2.29(3)	2.170	2.190
μ_{gs} [μ_N^2]	+0.702	+0.630	+0.911
$E_x(\frac{1}{2}_1^- \frac{1}{2})$	0.0	0.0	0.0
$E_x(\frac{3}{2}_1^- \frac{1}{2})$	3.685	2.501	0.886
$E_x(\frac{5}{2}_1^- \frac{1}{2})$	7.547	5.781	4.628
$E_x(\frac{1}{2}_2^- \frac{1}{2})$	8.860	8.702	8.135
$E_x(\frac{3}{2}_2^- \frac{1}{2})$	11.748	10.054	9.588
$E_x(\frac{7}{2}_1^- \frac{1}{2})$	12.438	14.244	9.795
$E_x(\frac{1}{2}_3^- \frac{1}{2})$		14.856	12.151
$E_x(\frac{3}{2}_1^- \frac{3}{2})$	15.108	15.210	13.592
$E_x(\frac{3}{2}_3^- \frac{1}{2})$		15.396	11.441
$E_x(\frac{5}{2}_2^- \frac{1}{2})$		15.764	12.756
$E_x(\frac{5}{2}_3^- \frac{1}{2})$		18.387	14.207
B(E2; $\frac{3}{2}_1^- \frac{1}{2} \rightarrow \frac{1}{2}_1^- \frac{1}{2}$)	6.4(15)	2.815	4.224
B(M1; $\frac{3}{2}_1^- \frac{1}{2} \rightarrow \frac{1}{2}_1^- \frac{1}{2}$)	0.70(7)	0.806	1.213

TABLE IX: Experimental and calculated energies, in MeV, ground-state point-proton rms radii, magnetic moments, as well as E2, in $e^2 \text{ fm}^4$, and M1, in μ_N^2 , transitions of ^{13}C . Results obtained using three-body effective interactions derived from the AV8' and AV8'+TM'(99) interactions are presented. A HO frequency of $\hbar\Omega = 15$ MeV was employed. Only experimental states known to be dominantly of p -shell character [37] are shown. The experimental values are from Ref. [23, 38].